ATLAS Internal Note
INDET-NO-171
16 June1997

Charge Collection Efficiency in Heavily Irradiated Silicon Diodes

L.Beattie, T.J.Brodbeck, A.Chilingarov, G.Hughes, P.Ratoff and T.Sloan
School of Physics and Chemistry
Lancaster University

Abstract

The Charge Collection Efficiency (CCE) has been measured for minimum ionising particles and for α-particle illuminations from both sides for planar diodes irradiated by neutrons and pions with fluences up to $3*10^{14}$ cm^{-2}. Geometrical effects in CCE for partially depleted detectors are deduced from the data as well as trapping effects for electron and holes separately.

1. Introduction

The diodes for the measurements described in this paper are the test structures (kindly provided by Liverpool University ATLAS group) produced by Micron Semiconductors together with strip detectors of various designs [1]. The diodes therefore can be regarded as typical in terms of the technology and materials used recently for microstrip detectors.

All the diodes were made from n-type Si. They have a sensitive area of 5x5 mm^2 surrounded by a guard ring and a thickness of ~300μm. Before irradiation their depletion voltages were between 10 and 30 volts.

The diodes were irradiated at two places: at ISIS(RAL) by neutrons with energy ~1MeV and at PSI(Villigen) by 300 MeV/c pions. The range of fluences used is (1-3)10^{14} cm^{-2}. All the irradiations were performed at room temperature and without bias. The fluence values for pions are used directly while those for neutrons are corrected to the equivalent fluences of 1MeV monoenergetic neutrons using hardness factor 1.1 taken from Ref.[2]. After the irradiation the diodes were kept at room temperature for several days until their depletion voltage ceased to decrease. After this the diodes were always kept at temperature below 10°C to avoid reverse annealing. This corresponds approximately to a situation expected in a real experiment where full beneficial annealing takes place while the reverse annealing is essentially suppressed [3]. Further details about the diodes and their irradiation are presented in Table 1.

The CCE measurements have been so far performed for 4 diodes (2 irradiated by pions and 2 irradiated by neutrons) covering the whole range of the fluences used. The different diodes are at different stages of characterisation at the moment. More data as well as a more detailed analysis will follow shortly.

1. Depletion Voltage

The depletion voltage was measured with the help of an HP-4263A LCR meter. Before irradiation the measurements were performed at room temperature; after irradiation they were performed at 0°C. A frequency of 10 kHz was chosen as a standard for the CV measurements. The value of the depletion voltage was defined by the crossing of two straight lines in the logC-logV plot. The details of these measurements can be found in Ref.[4]. The error on an individual measurement of the depletion voltage was estimated to be ~5%.

As shown in [4], the depletion voltage measured at 1kHz is higher by 10-15% than that measured at 10kHz. This was observed for all temperatures in the range -16° - +32°C. This indicates the order of magnitude of systematic effects in this method of depletion voltage measurement. Efforts to understand these effects are continuing in the Lancaster group.

The change of the depletion voltage vs. fluence is presented in Fig.1. Since type inversion has occurred for all diodes at these fluences [3], the change in the depletion voltage is a sum of the final and initial depletion voltages: $U_d^{fin} + U_d^{init}$. All the data are corrected to a standard thickness 300 μm. The lines show the expected area calculated from the results of a world data survey performed in [3]. Practically all the points lie within the expected zone. One can also see that the damage produced by 300 MeV/c pions is very close to that produced by 1MeV neutrons, in agreement with earlier observations [5].

2. Set-Up for CCE Measurements

Charge collection efficiencies were measured for minimum ionising particles (MIP) and 5MeV α-particles with the help of a fast amplifier, BIPOLTEST[6], with a shaping time of ~25 ns that matches the front-end electronics to be used for the ATLAS Semiconductor Tracker[7]. The very large dynamic range of BIPOLTEST allows the detection of MIPs and α-particles with the same preamplifier. With a diode connected to the amplifier input the noise was < 3000 electrons.

MIP CCE measurement were performed using a collimated ^{90}Sr β-source. A coincidence between 2 scintillator counters installed one after another behind the test diode was used as a trigger. This suppressed bremsstrahlung photon background and allowed selection of β-particles with γ-factor ~5 i.e. real MIPs. In measurements with α-particles and ^{57}Co gammas the trigger from the detector signal itself was used. The preamplifier and scintillator counters are situated inside the refrigerator with an external thermocontrol allowing the temperature of the system to be set at any value

between -25° and +20°C with ~1°C variations. Further details of the set-up can be found elsewhere[8,9].

A typical MIP spectrum is shown in Fig.2 together with the corresponding Landau fit. The good quality of the trigger is illustrated by the absence of false triggers that should appear as a pedestal peak around channel 13 of the histogram. This shows also that our system has no lower limit in measurement of CCE values for MIPs.

A typical spectrum for α-particles is presented in Fig.3. The large signal in this case allowed self-triggered CCE measurements down to a few percent level. The peak position was found by a gaussian fit also shown in the Fig.3. Gamma quanta from a ^{57}Co radioactive source with 122 keV energy were used for the absolute calibration of the system. A typical ^{57}Co spectrum is shown in Fig.4. The photopeak position was determined by a gaussian fit as shown in the histogram.

Before the irradiations all the measurements were performed at room temperature, but after irradiations a temperature of +10° or 0°C was used in order to suppress the dark current and to prevent the reverse annealing during the measurement period. Note that the operation temperature for ATLAS SCT is expected to be between 0° and -10°C.

3. CCE Results

For each diode, the most probable value of the Landau distribution Δ_{mp} was measured before irradiation at 100 and 120V bias. Within ~1% statistical errors the results at those two voltages agree. For a few diodes it was verified that further increase of the voltage also did not change the result. Normalising Δ_{mp} by the calculated value of dE/dx=270 eV/μm[8] allowed a measurement of the diode thickness. It was checked that with ~2% accuracy this thickness agrees with a nominal wafer thickness available for some of the diodes.

The MIP CCE for the irradiated diodes was defined as the ratio between Δ_{mp} observed after irradiation to the value of Δ_{mp} before the irradiation. A complete Landau fit with gaussian smearing was essential because the visible peak position of the smeared Landau distribution depends on the noise, which was different for the diodes before and after the irradiation due to the large increase of the dark current, especially at highest voltages used. The maximum voltage was limited either by the hardware limit of 500V or by the diode breakdown.

The response of the diodes to the α-particles for the front and back side illuminations was measured for several diodes before the irradiation. The results for different diodes agreed within the ~2% accuracy corresponding to the long term stability of the system, and their average value was used for all the diodes to calculate the α-particle CCE after irradiation. The latter was defined as the ratio of peak position in the α-spectrum to its nominal value for the non-irradiated diode.

Measured values of the CCE for MIPs and α-particles for the back side illumination vs. bias voltage U_{bias} are presented in Fig.5. Separately the CCE for the α-back

illumination are presented in Fig.6 vs. square root of U_{bias}. Fig.7 shows CCE for MIPs and both side α-illuminations vs. U_{bias} above the depletion voltage for each diode. The drawing in Fig.8 explains the notation used for the diode description.

4. Discussion of the CCE Results

As can be seen from Figs.5,6 for a bias voltage lower than the depletion voltage the MIP CCE grows linearly with bias voltage while the α-particle back side CCE is proportional to the square root of U_{bias}. This can be interpreted as follows.

It has been known for a long time [10] that the response of heavily irradiated Si to an AC electrical signal with a period shorter than few microseconds is the same for the depleted and non-depleted part of the Si bulk, both parts behaving as an insulator. This is due to the fact that conductivity in heavily irradiated Si is provided by the deep level defects rather than by shallow level dopants as in the non-irradiated Si. In this sense, the heavily irradiated Si is very similar to a semi-insulating GaAs.

As a result for both of these materials the non-depleted bulk acts as an insulator for a fast electrical signal produced by the drift of electrons and holes released in the active (depleted) part of the detector. For typical bias value of ~200V and a typical thickness of ~300μm the collection time does not exceed 10 ns. Therefore the signal development in a detector made of such a material is as follows. The ionisation released in the depleted region drifts to the junction electrode and to the edge of the non-depleted (or low electric field) region corresponding to the sign of the carriers. During this drift the signal charge is induced directly on the p^+ and n^+ electrodes of the detector by the carrier electric field penetrating through the non-depleted bulk just as it does through the depleted part of the detector. This fast phase of the collection process ends when the drift of all the carriers released in an active part of the detector is finished (normally in less than 10 ns). After this a slow phase starts during which the carriers stuck near the edge of the non-depleted area are neutralised by the free carriers arriving from the electrically neutral bulk. As estimated in [11], the characteristic time for this process in Si is of order of 400ns.

For a planar diode and the fast front-end electronics used in our case the above considerations plus the Ramo theorem[12] predict that in a partially depleted detector the signal from α-back illumination will be proportional to the ratio of the active region thickness d to the full detector thickness w. For a uniform space charge this ratio in turn should be equal to $(U_{bias}/U_{dep})^{1/2}$. For MIPs this is also valid, but additionally the amount of the initially released ionisation is proportional to the active thickness d. Therefore the MIP CCE should be proportional to $(d/w)^2$ or to the bias voltage U_{bias}.

If carriers are partially trapped during their drift the CCE does not reach 100% even when U_{bias} reaches U_{dep}. The following considerations can explain why this "trapping attenuation" may be almost independent of the bias voltage in a partially depleted detector. In the usual approximation trapping is a function of the ratio of the collection time to the carrier lifetime. Since in a partially depleted detector the drift field goes

down to zero at the end of the depleted region the full collection time is meaningless since it diverges logarithmically[8]. Instead a characteristic collection time should be used which can be estimated as a ratio of d to an average drift velocity <v>. Without saturation <v> is proportional to the average drift field U_{bias}/d. Therefore the characteristic collection time is proportional to d^2/U_{bias} and does not depend on U_{bias}, if the latter is proportional to d^2 as was discussed in the previous paragraph. Together with collection time the trapping does not change with U_{bias} (if the lifetime is not influenced by the bias voltage).

When bias voltage exceeds U_{dep} the collection time decreases with the voltage. Thus the attenuation due to trapping can be reduced by a voltage increase as can be seen from Fig.7. The information presented in this figure is sufficient to extract the lifetime for electrons and holes separately and to check whether they can be considered as independent of the bias voltage. This analysis (complicated by the so called plasma effects[13] for the α-particle signals) is now in progress and will be reported elsewhere [14]. The lines in Fig.7 show examples of the fits performed. The preliminary results of this analysis show that in practically all situations the electron and hole contributions to the MIP signal are very close. Therefore our MIP CCE results for the planar diodes can be regarded with a reasonable accuracy as valid also for a finely segmented detector with any type of electrodes.

CCE for MIP and α-particle back side illumination measured at the depletion voltage are presented in Table 2 vs. U_{dep} and in Fig.9 vs. fluence. For each diode the MIP and α-particle CCEs are very close. This indicates again the similarity in the hole and electron trapping. Neither CCE decreases very much with fluence because the decrease in carrier lifetimes is partially compensated by the decrease in the effective collection time due to the increase in the applied voltage. In Fig.10 the MIP CCE at a fixed bias voltage above U_{dep} is shown as a function of fluence for several bias voltages. In this case a rather steep decrease of the signal with fluence is obvious. The scale of the effect agrees with earlier observations[5,15].

5. Conclusions

The CCE measurements show that in a partially depleted planar diode the MIP signal is proportional to the bias voltage while the α-particle signal for the n^+-side illumination is proportional to the $(U_{bias})^{1/2}$. This can be consistently interpreted as a result of the following phenomena:
a) the depleted area grows with voltage from the n^+ electrode (p-type Si);
b) the active (depleted) thickness of the detector grows proportionally to the $(U_{bias})^{1/2}$;
c) non-depleted part of the heavily irradiated Si detector is transparent for the fast electrical signals produced by the drift of carriers released by an ionising particle;
d) signal attenuation due to carrier trapping in a partially depleted detector is almost independent of the bias voltage.

For a fluence range $(1\text{-}3)10^{14}cm^{-2}$ MIP CCE at the depletion voltage depends weakly on the fluence, while for any fixed bias voltage above the depletion voltage the CCE decreases with fluence rather steeply.

Acknowledgments

The authors would like to express their gratitude to B.K.Jones and J.Santana for helpful discussions and to S.Holt and D.Campbell for technical support. The help from M.Edwards and D.Hill from RAL in performing the neutron irradiations and from K.Gabathuller (PSI) in performing the irradiations by pions is gratefully acknowledged.

REFERENCES

1. J.D.Richardson, PhD thesis, University of Liverpool, 1995.
2. T.Angelescu and A.Vasilescu, *Nucl.Instr.and Meth.* **A374**(1996)85.
3. A.Chilingarov et al., *Nucl.Instr.and Meth.* **A360**(1995)432.
4. L.Beattie et al., ROSE (RD-48) Technical Note 97/4, March 1997.
5. S.J.Bates et al., *Nucl.Instr.and Meth.* **A379**(1996)116.
6. P.Jarron et al., in: "New Technologies for Supercolliders", eds. L.Gifarelli and T.Ypsilantis (Plenum, New York,1991) pp. 105-123.
7. CERN LHCC/97-17; ATLAS TDR 5. 30 April 1997.
8. S.Bates et al., *Nucl.Instr.and Meth.* **A337**(1993)116.
9. A.Chilingarov and T.Sloan, Proc.of the 3rd Int.Workshop on Gallium Arsenide and Related compounds, San Miniato, Italy, March 21-24 1995, World Scientific, p.52.
10. Z.Li and H.W.Kraner, IEEE Trans. on Nucl.Sc. **NS-38**(1991)244.
11. G.Lutz, *Nucl.Instr.and Meth.* **A377**(1996)234.
12. S.Ramo, IRE **27**(1939)584.
13. R.N.Williams and E.M.Lawson, *Nucl.Instr.and Meth.* **120**(1974)261.
14. T.J.Brodbeck et al. "Carrier lifetimes in heavily irradiated Si diodes", ATLAS INDET Note (in preparation).
15. F.Lemeilleur et al., *Nucl.Instr.and Meth.* **A360**(1995)438.

TABLES

Table 1. Diode and irradiation details.

Diode #	Irrad. type	Fluence, 10^{14} cm^{-2}	Thickness, μm	Initial U_{dep},V	Irrad. time,d	Anneal. time,d	Final U_{dep},V
4	pion	1.15±0.07	304	10.2	2	6.5	179
14	pion	1.26±0.07	300	12.7	2	6.5	209
32	pion	2.50±0.09	301	12.5	4	4.5	313
28	pion	2.65±0.08	294	13.4	4	3.5	309
9	neutron	1.07±0.08	297	15.0	1.8	8.0	161
41	neutron	1.07±0.08	303	33.5	1.8	7.0	143
7	neutron	1.32±0.11	296	14.5	3.2	5.0	268
42	neutron	1.32±0.11	298	33.6	3.2	4.0	211
13	neutron	2.14±0.10	303	12.9	4.2	5.0	324
49	neutron	2.14±0.10	307	14.5	4.2	2.0	319
46	neutron	2.75±0.18	314	14.6	5.0	2.0	386

Table 2. CCE for MIPs and α-particle back side illumination at the depletion voltage.

Diode #	U_{dep},V	MIP CCE,%	α-back CCE,%
41	143	78.4±1.6	73.4±1.5
14	209	76.8±1.5	73.1±1.5
28	309	61.2±1.2	62.3±1.3
46	386	71.9±1.4	69.6±1.4

FIGURE CAPTIONS

Fig.1. Change in the depletion voltage ($U_d^{fin} + U_d^{init}$) corrected to 300 μm diode thickness vs. fluence in units of 10^{14} cm^{-2} for pion (shaded symbols) and neutron (open symbols) irradiations. The lines show the area of expected values calculated from the results of world data survey performed in [3].

Fig.2. Typical MIP spectrum with Landau fit. Pedestal position is 13.2 histogram bins.

Fig.3. Typical α-particle spectrum with gaussian fit.

Fig.4. Typical ^{57}Co spectrum with gaussian fit.

Fig.5. MIP (shaded symbols) and back side α-particle (open symbols) CCE vs. U_{bias} for diodes irradiated by neutrons a),b) and by pions c),d). For α-particles the points are connected by the line to guide the eye. For MIPs the linear fit is made through the points below the depletion voltage. The plots refer to: a) diode #41, U_{dep}=143V, fit for U_{bias} up to 140V; b) diode #46, U_{dep}=386V, fit for U_{bias} up to 380V; c) diode #14, U_{dep}=209V, fit for U_{bias} up to 200V; d) diode #28, U_{dep}=309V, fit for U_{bias} up to 300V.

Fig.6. The CCE for α-particle illumination from the back side vs. square root of U_{bias} (in V). The linear fit is made through the points below the depletion voltage. The Fig.6a shows the diodes irradiated by neutrons, Fig.6b - those irradiated by pions.

Fig.7. MIP (crosses) and α-particle CCE for the back (diamonds) and the front (squares) illuminations for the bias above the depletion voltage. For α-particles the errors are within symbol size. The assignment of the figures is the same as in Fig.5. The fit lines are shown for the points included in the fit.

Fig.8 Schematic diagram of the diode after the type inversion. The non depeleted area of the detector is shaded.

Fig.9. MIP (shaded symbols) and back side α-particle CCE (open symbols) at the depletion voltage vs. fluence in units of 10^{14} cm^{-2}.

Fig.10. MIP CCE vs. fluence in units of 10^{14} cm^{-2} for several fixed bias voltages above the depletion voltage. The lines are drawn to guide the eye.

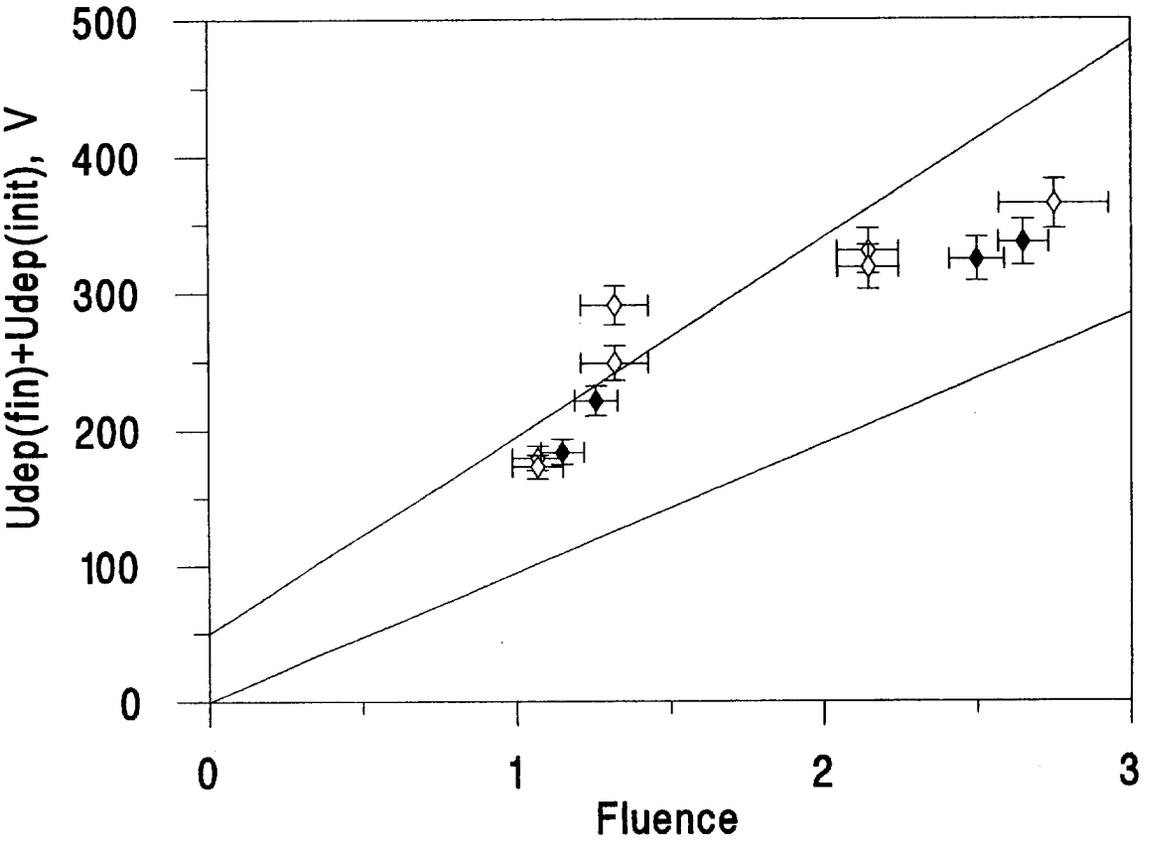

Fig.1

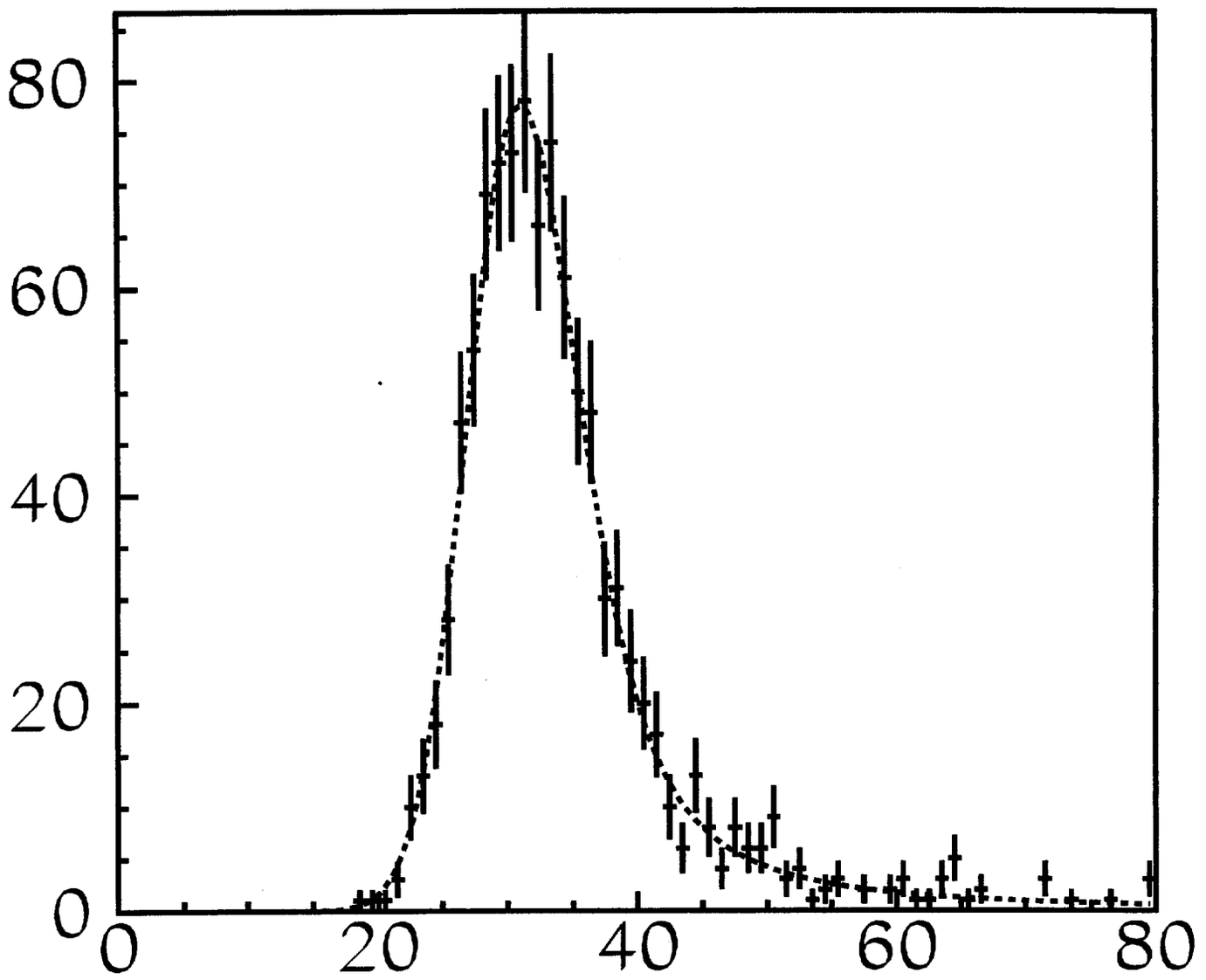

Fig. 2

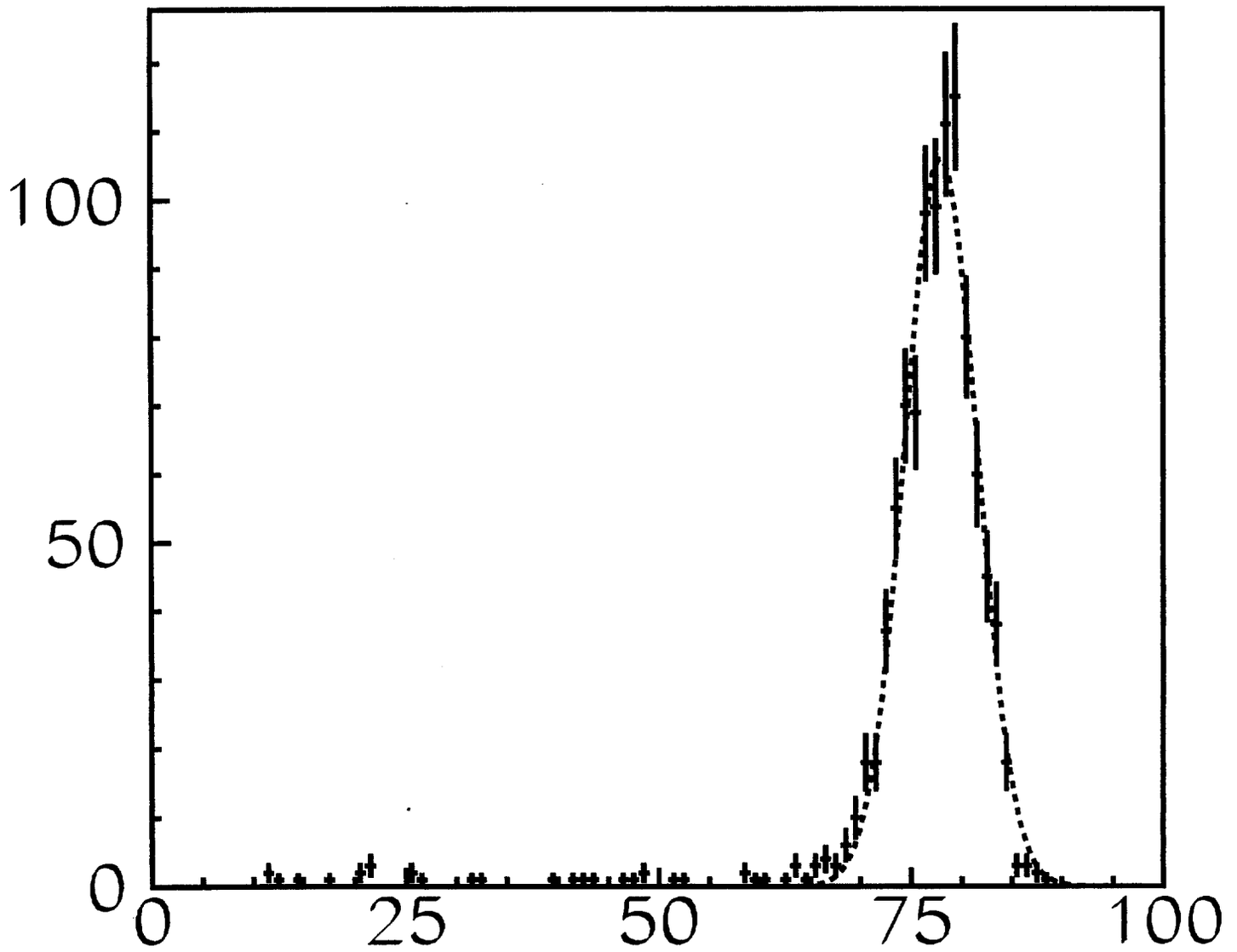

Fig. 3

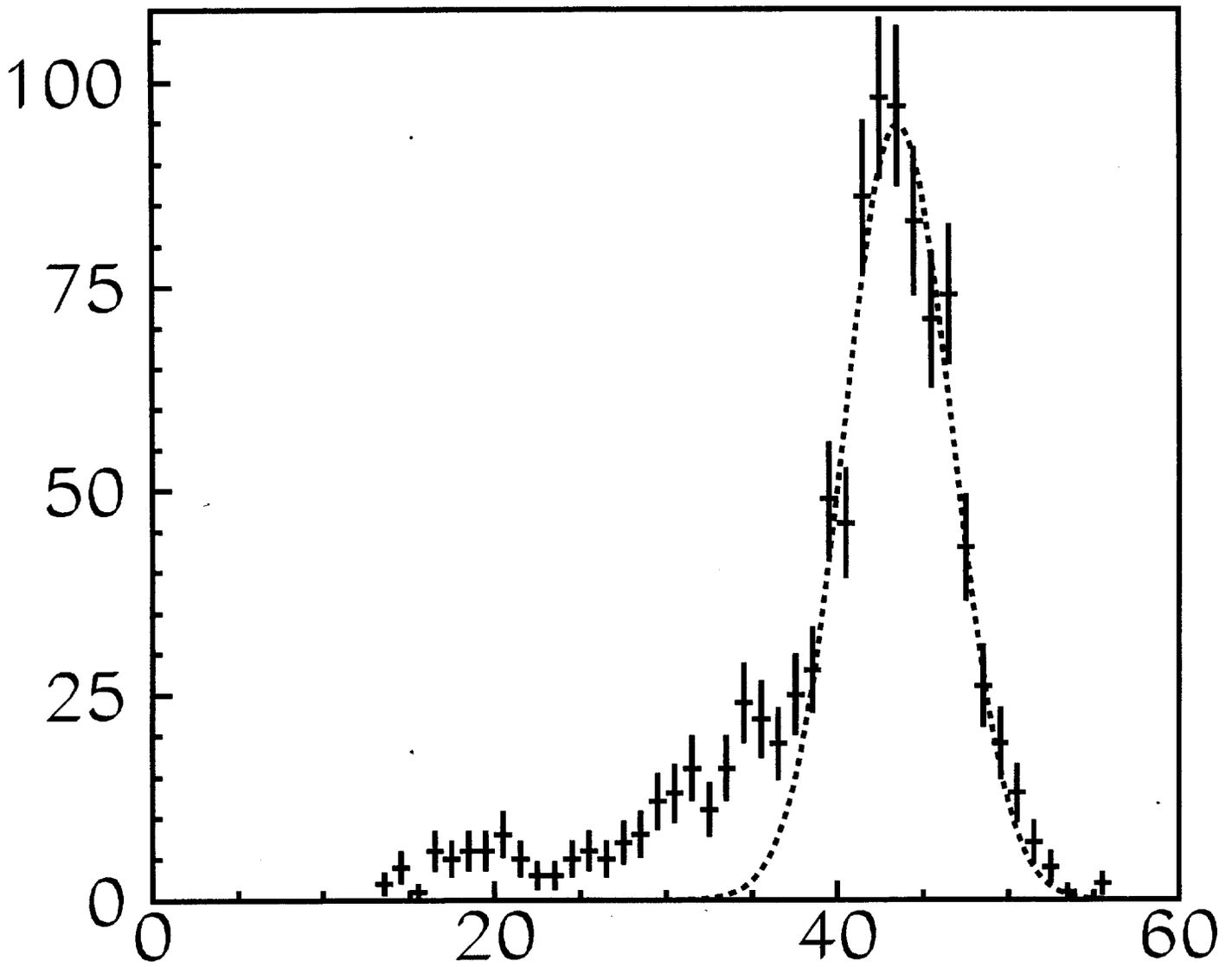

Fig. 4

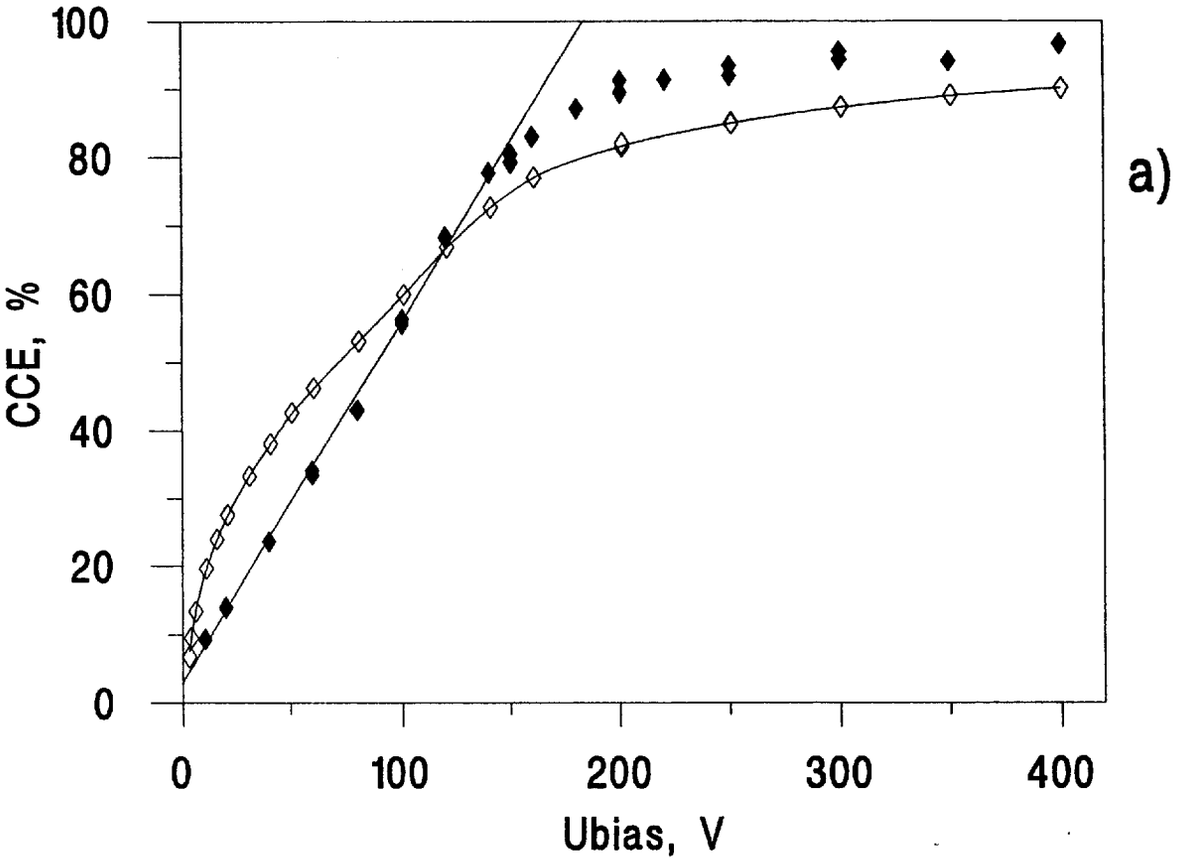
100
80
60
40
20
0
CCE, %
0
100
200
300
400
Ubias, V
a)

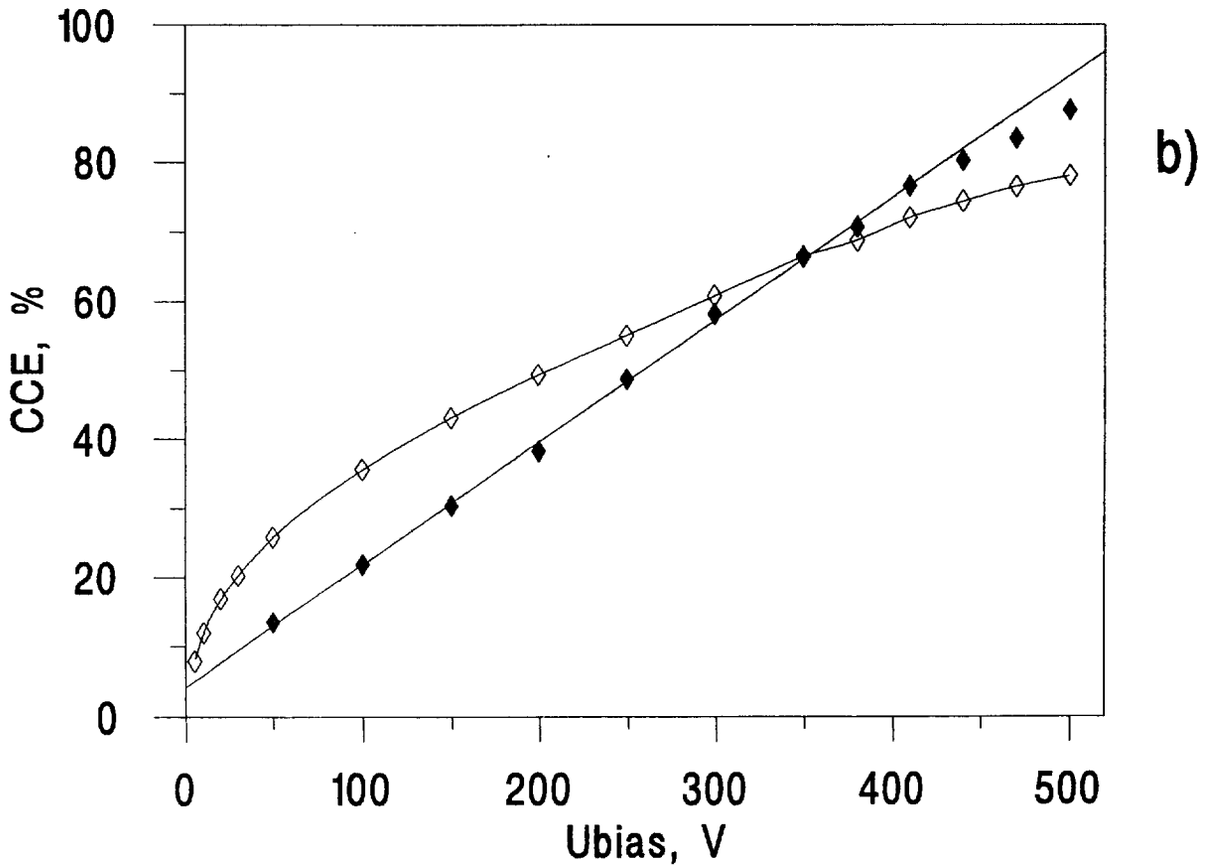
100
80
60
40
20
0
CCE, %
0
100
200
300
400
500
Ubias, V
b)

Fig.5

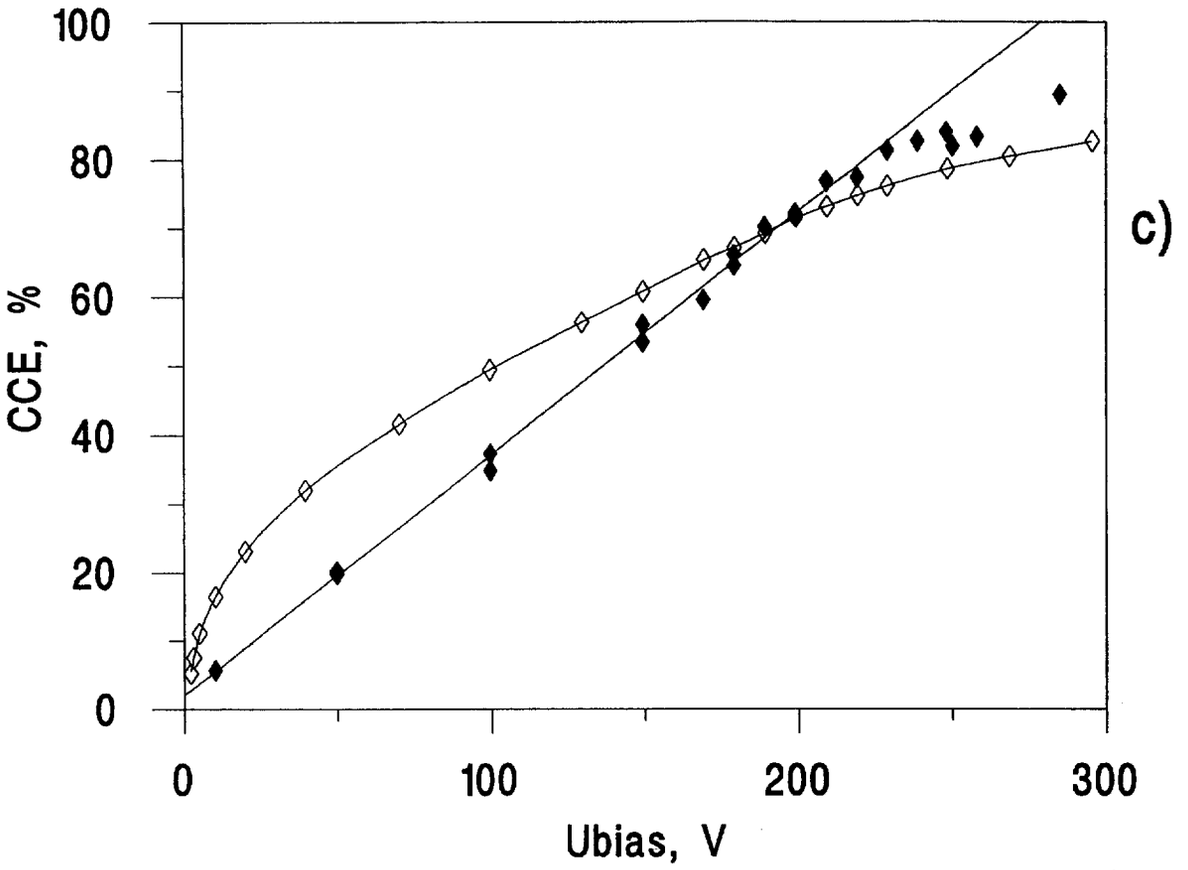
100
80
60
40
20
0
CCE, %
0
100
200
300
Ubias, V

c)

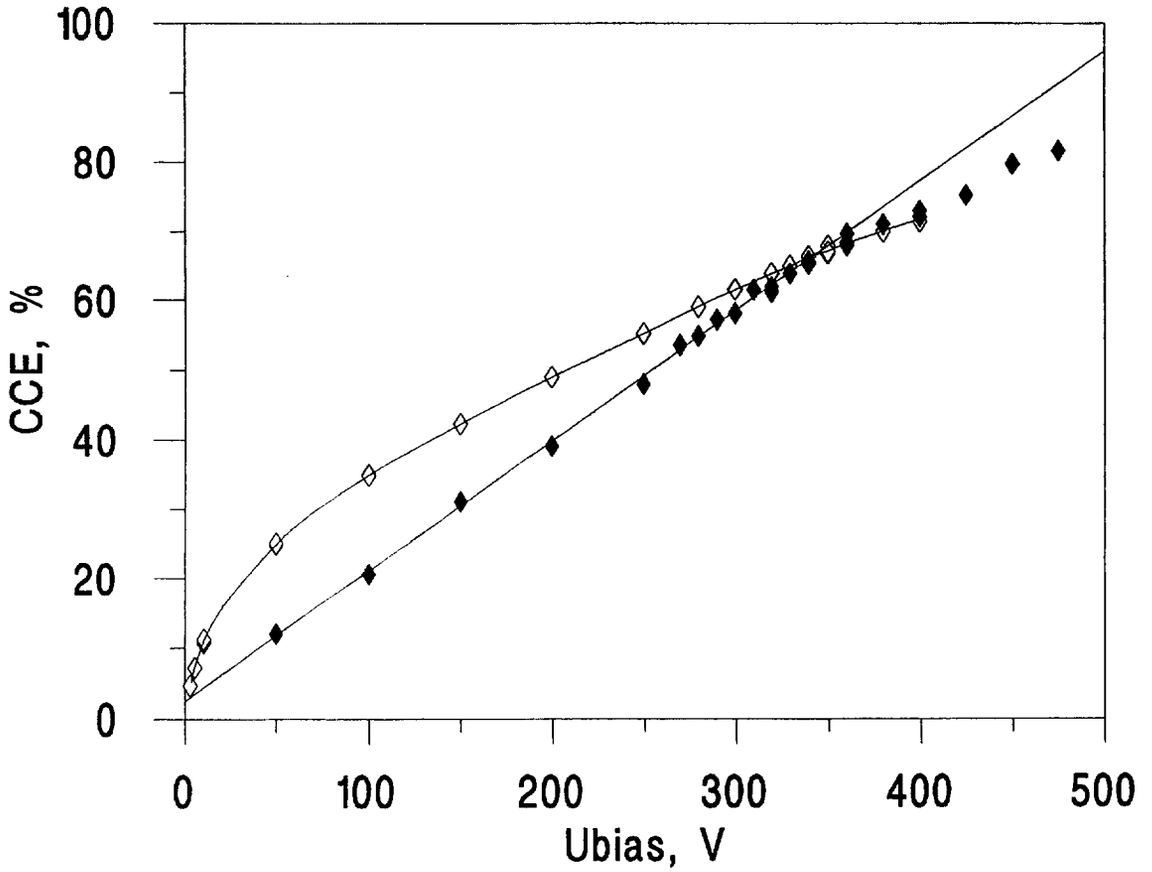
100
80
60
40
20
0
CCE, %
0
100
200
300
400
500
Ubias, V

d)

Fig.5

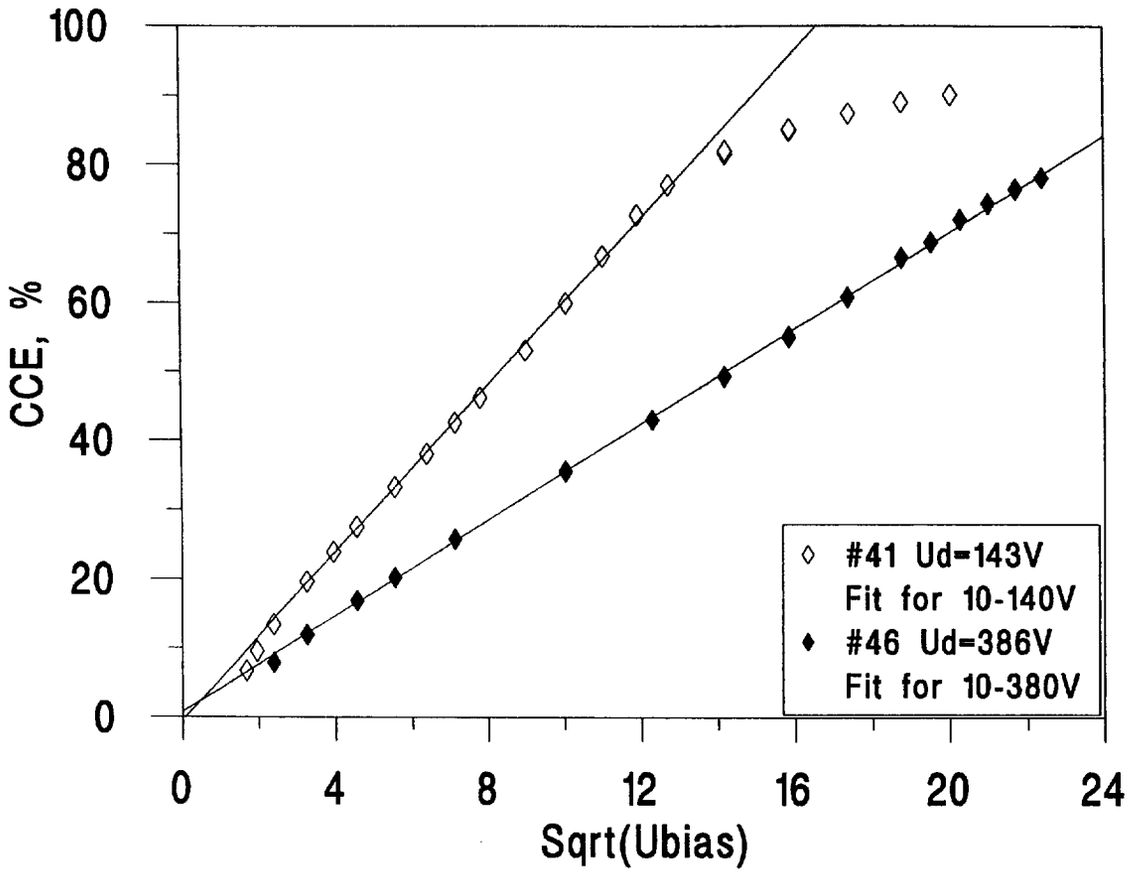
100
80
60
40
20
0
CCE, %
0
4
8
12
16
20
24
Sqrt(Ubias)
#41 Ud=143V
Fit for 10-140V
#46 Ud=386V
Fit for 10-380V

a)

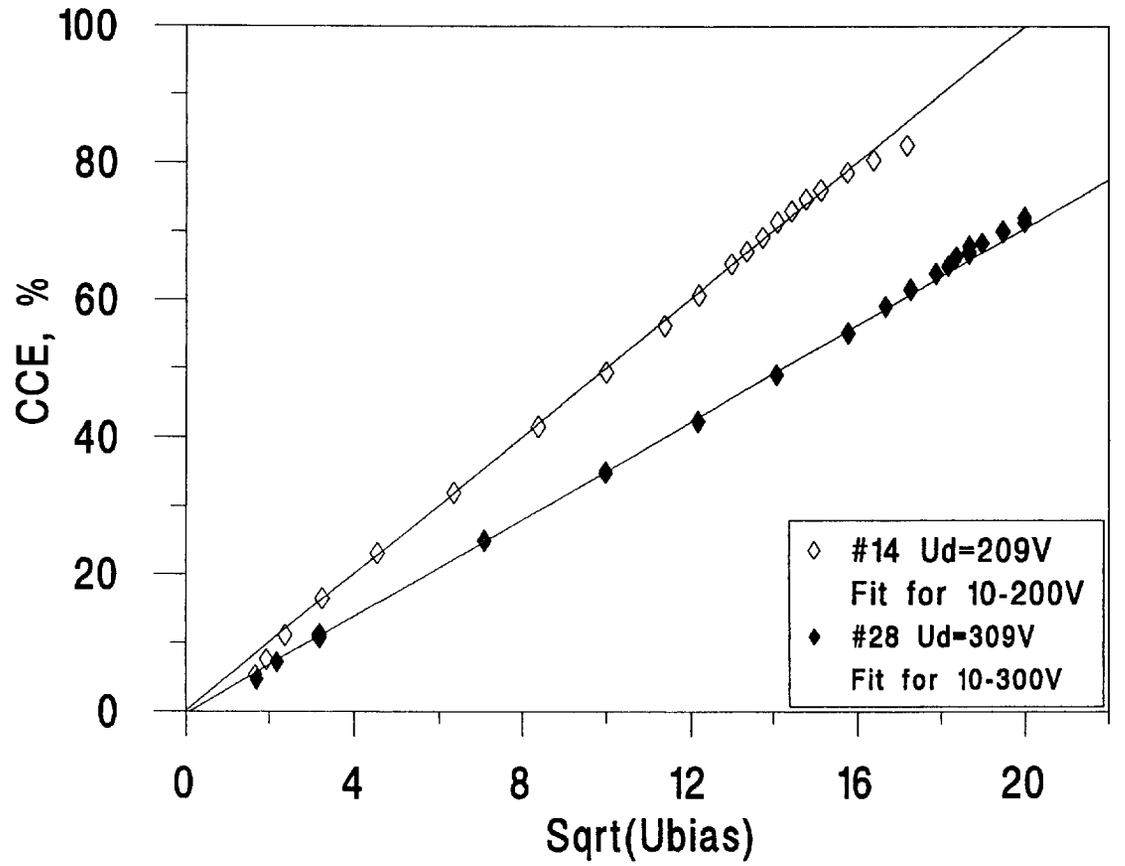
100
80
60
40
20
0
CCE, %
0
4
8
12
16
20
Sqrt(Ubias)
#14 Ud=209V
Fit for 10-200V
#28 Ud=309V
Fit for 10-300V

b)

Fig.6

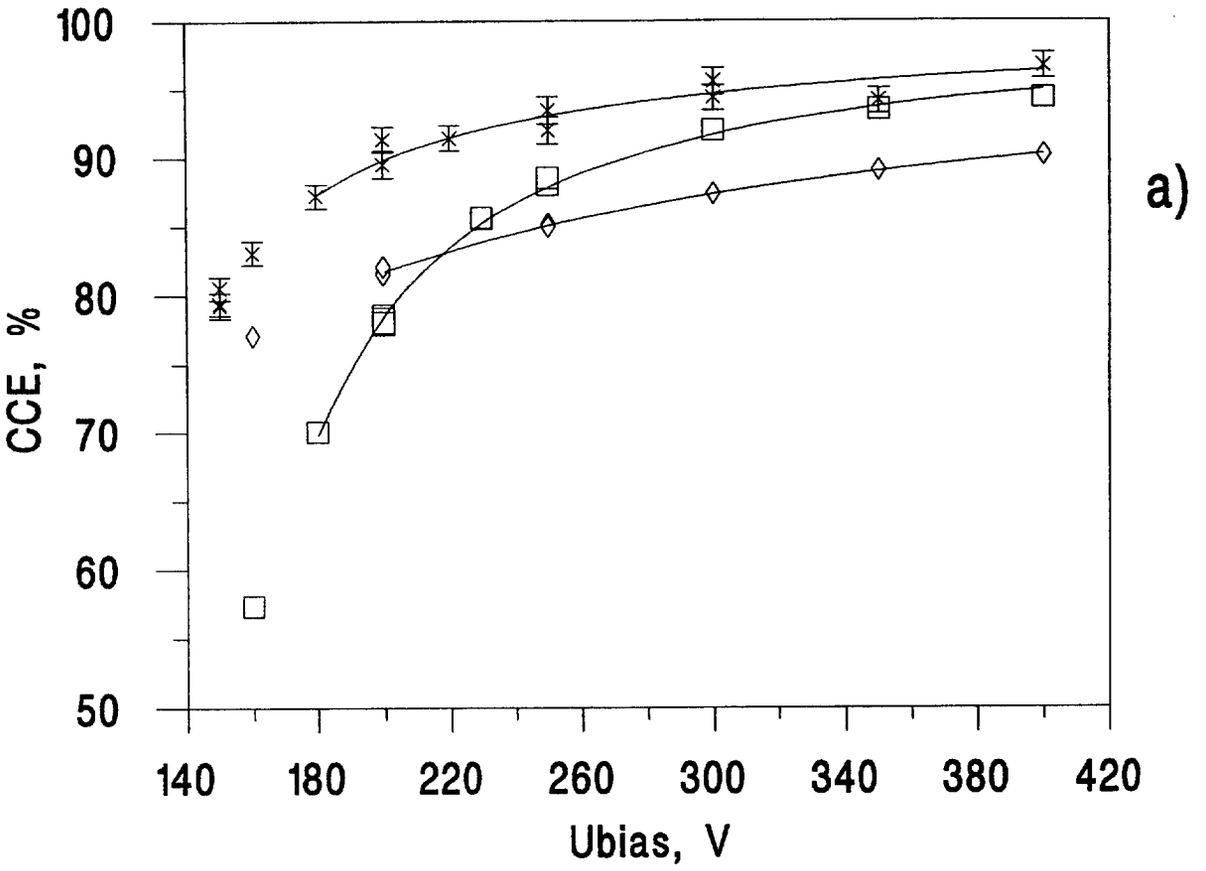
100
90
80
70
60
50
CCE, %
140
180
220
260
300
340
380
420
Ubias, V

a)

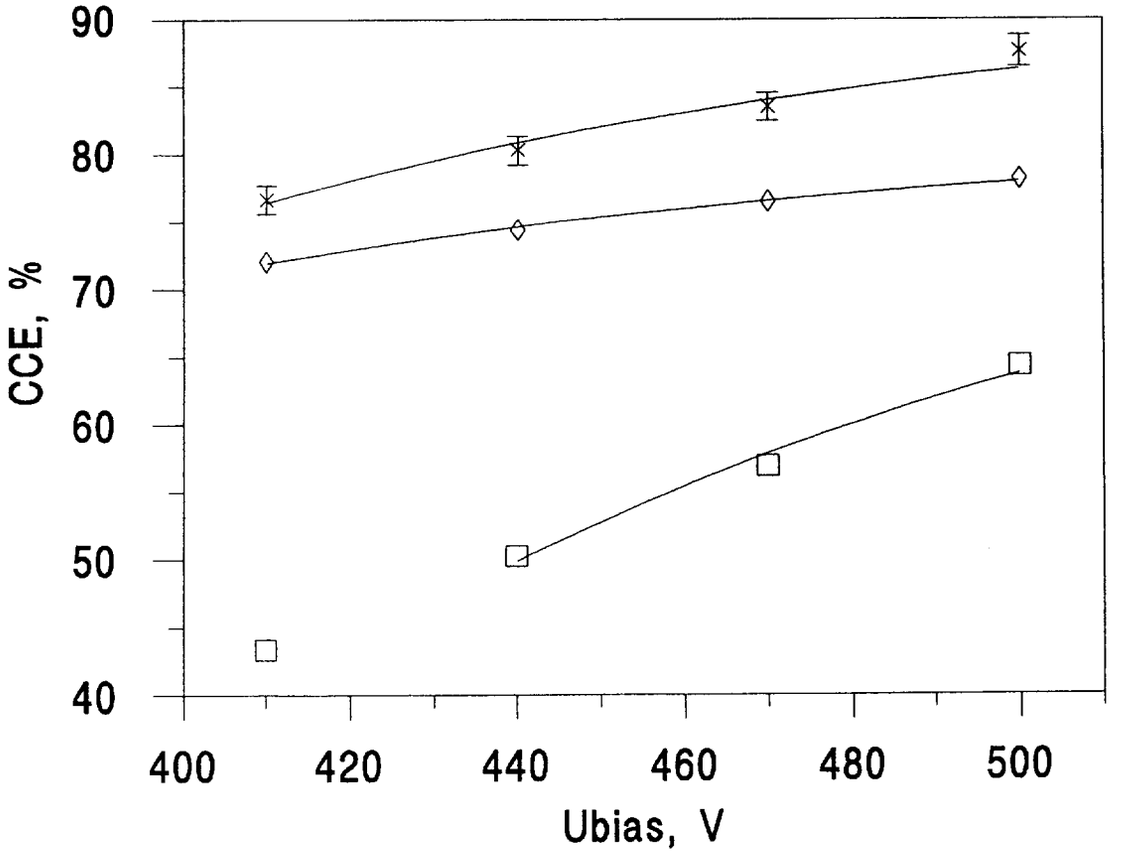
90
80
70
60
50
40
CCE, %
400
420
440
460
480
500
Ubias, V

b)

Fig.7

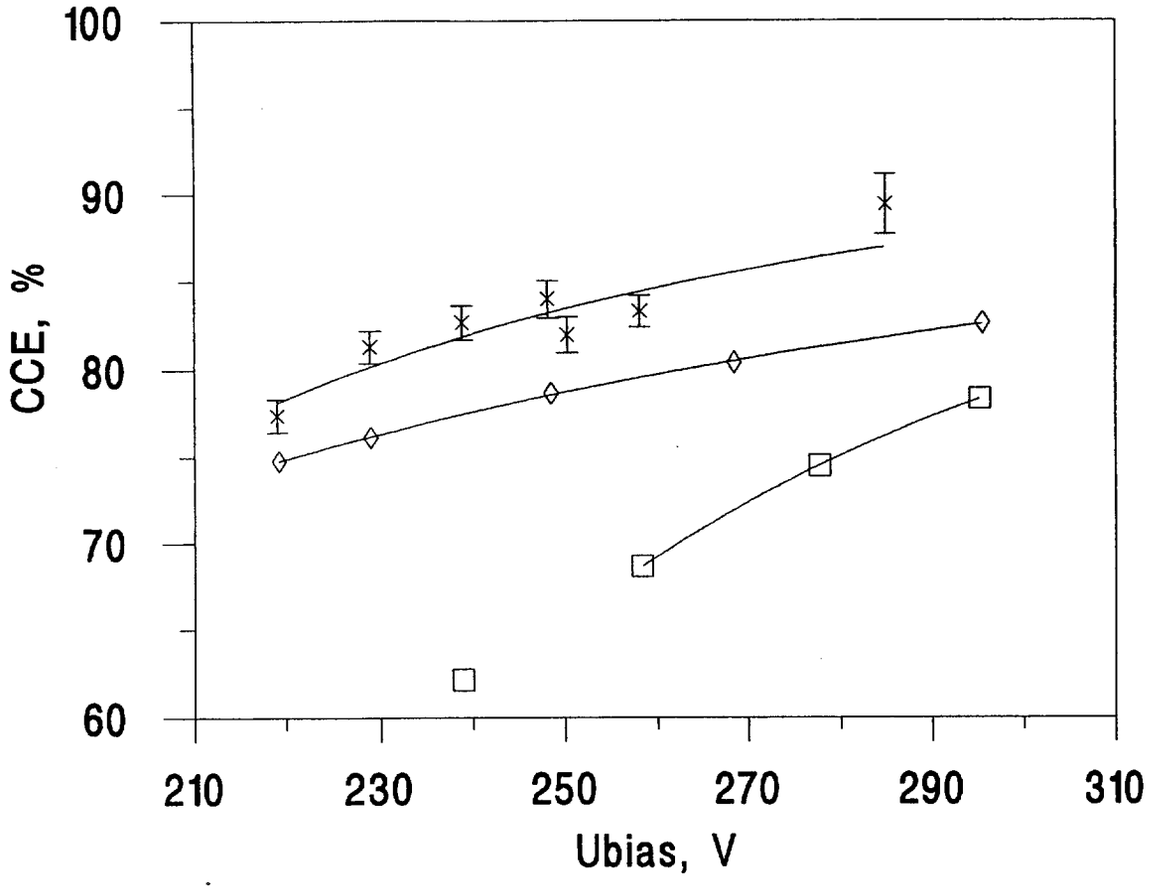
100
90
80
70
60
CCE, %
210
230
250
270
290
310
Ubias, V

c)

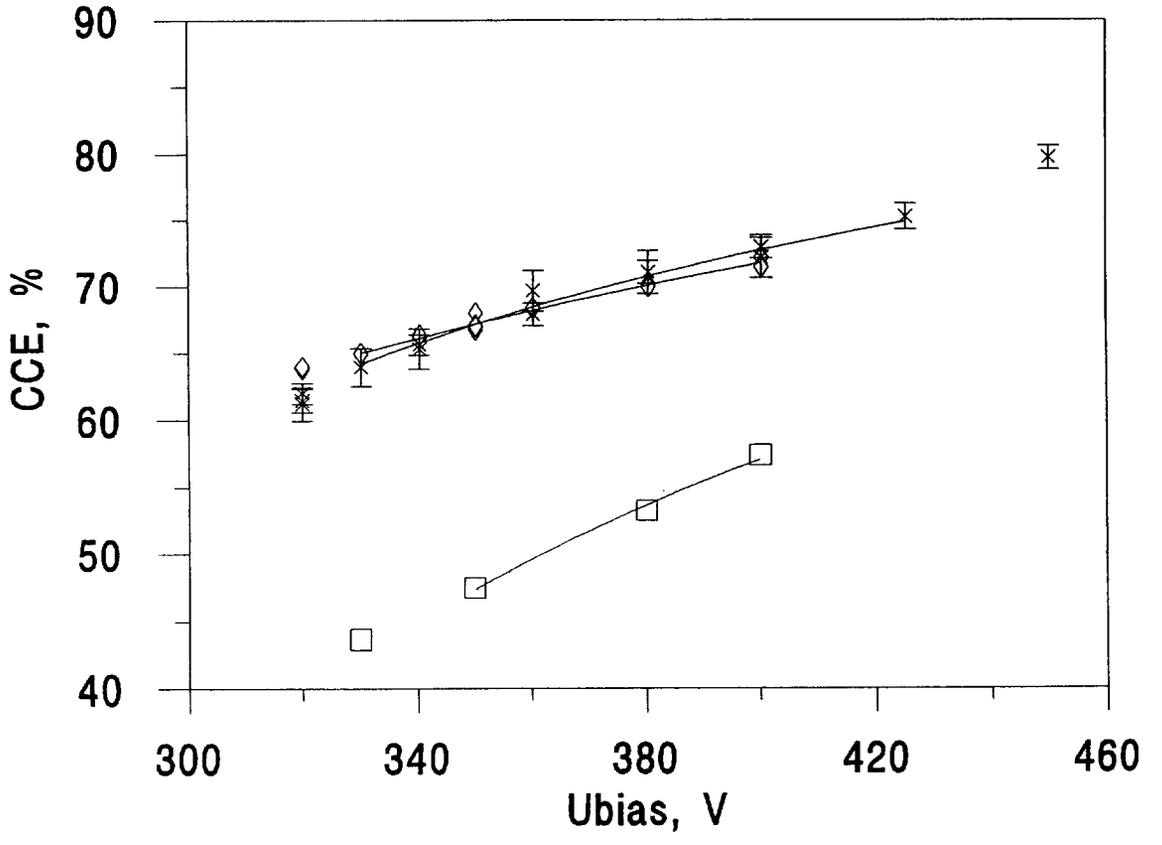
90
80
70
60
50
40
CCE, %
300
340
380
420
460
Ubias, V

d)

Fig.7

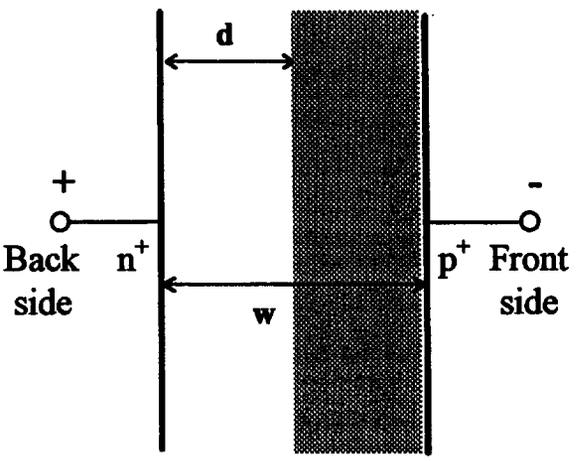

Fig.8

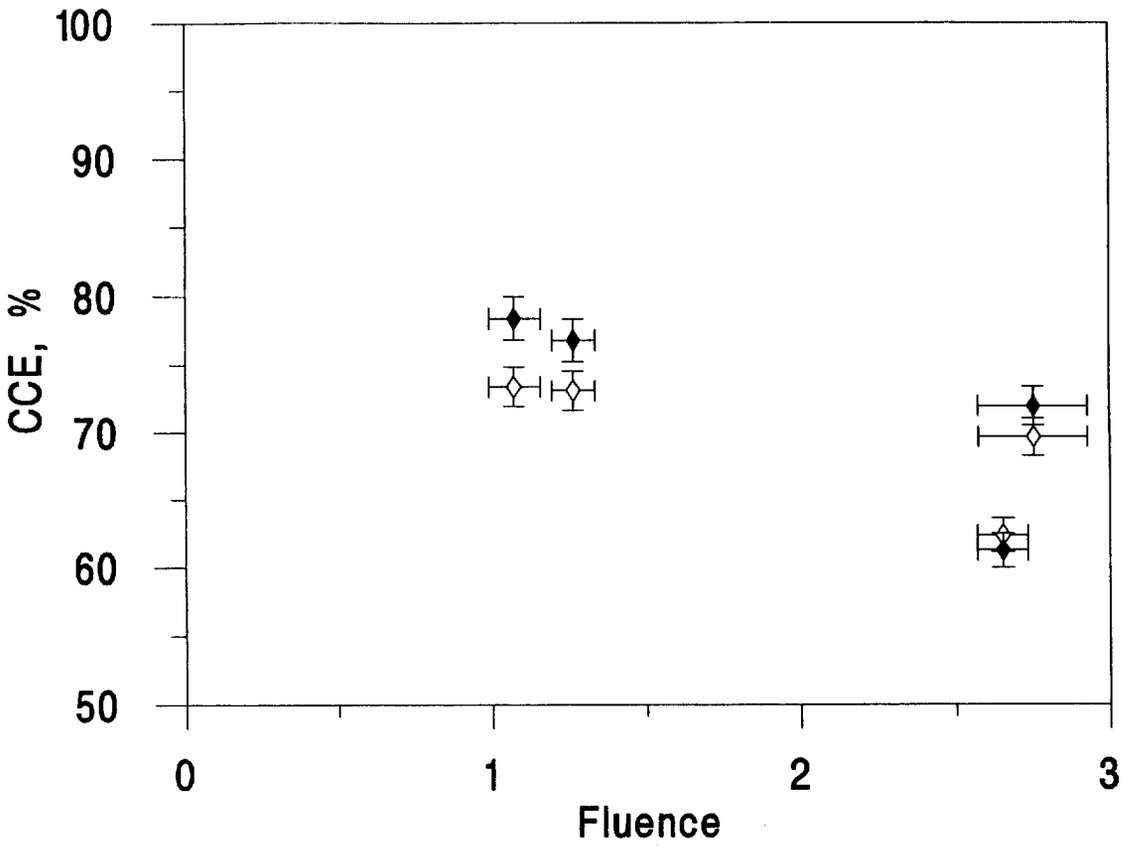
100
90
80
70
60
50
CCE, %
0
1
2
3
Fluence

Fig.9

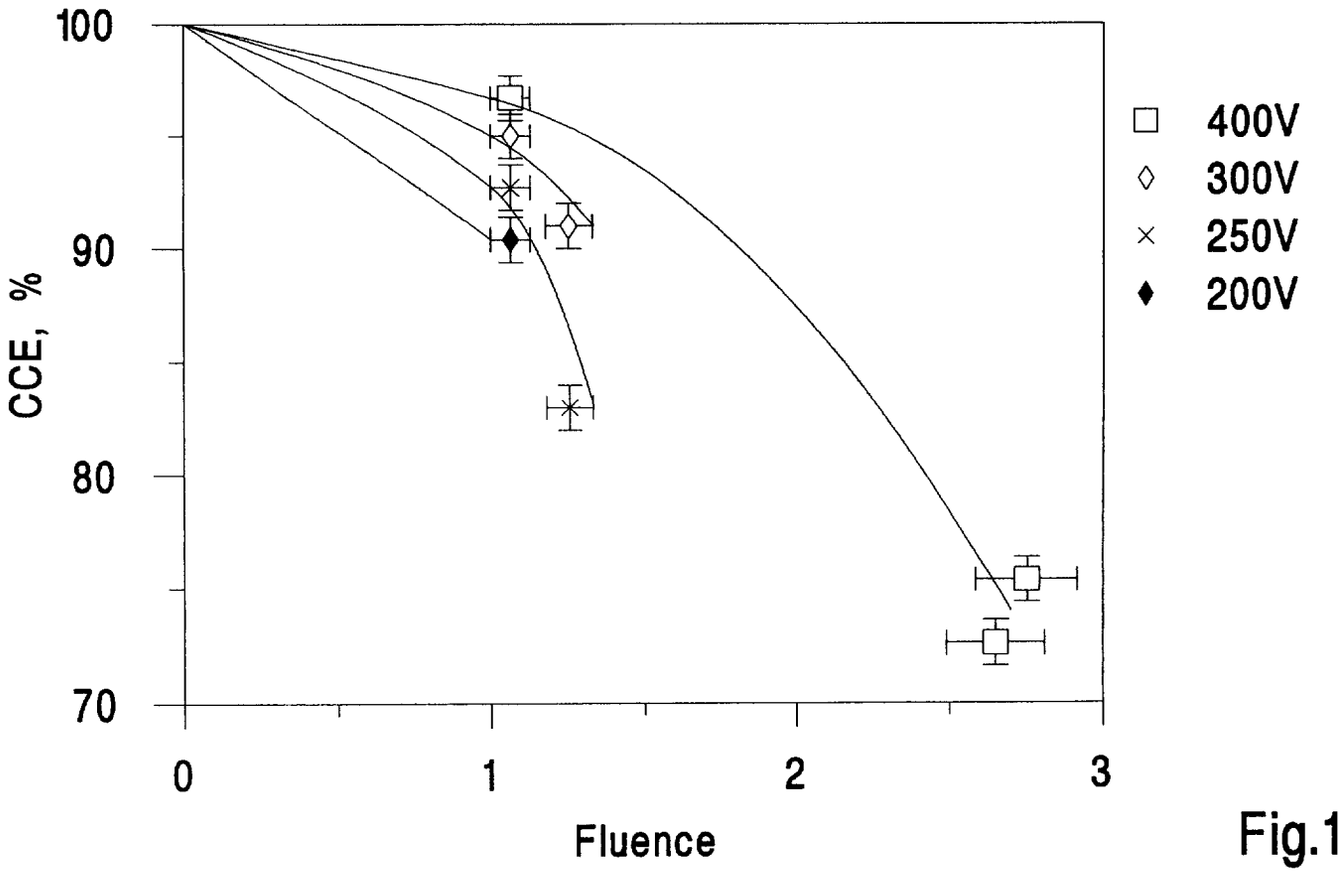
100
90
80
70
CCE, %
0
1
2
3
Fluence
400V
300V
250V
200V

Fig.10